RSC Advances

PAPER

Cite this: RSC Adv., 2018, 8, 30502

A novel nanofiltration membrane inspired by an asymmetric porous membrane for selective fractionation of monovalent anions in electrodialysis†

Jincheng Ding,[a] Shanshan Yang,[a] Jiefeng Pan,*[ab] Yu Zheng,[a] Arcadio Sotto[c] and Jiangnan Shen *[a]

The present study describes the synthesis of new nanofiltration membranes inspired by asymmetric porous membranes used as monovalent anion selective membranes for electro-membrane separation. The membrane surface was firstly modified, by deposition of a mussel-inspired "bio-glue" polydopamine (PDA) layer, and subsequently a compact polyamide layer was polymerized on the surface of the membrane's active layer. The chemical constitution and structure of these modified porous membranes were explored by Fourier transform infrared spectroscopy (FT-IR) and scanning electron microscopy (SEM). The surface roughness and hydrophilicity of the membranes were explored by atomic force microscopy (AFM) and water contact angle measurements, respectively. In addition, the electrochemical properties of the surface of the modified membranes were analyzed in terms of membrane surface resistance and zeta potential values. As for the performance of these modified porous membranes, this was investigated by measuring the permselectivity of a Cl^-/SO_4^{2-} system. The obtained results show that the new membranes exhibit an enhanced monovalent anion permselectivity, which is in agreement with the improved membrane surface properties. Furthermore, membranes modified by the addition of a PDA layer and a dense polyamide active layer lead to a significant improvement in selectivity $\left(P^{Cl^-}_{SO_4^{2-}} = 3.1\right)$, compared with a conventional interfacial polymerization modified membrane $\left(P^{Cl^-}_{SO_4^{2-}} = 1.42\right)$. The excellent performance can be ascribed to the synergistic effect of the compact PDA layer and negatively charged interfacial polymerization layer, dependent on the sieving and electrostatic repulsion, respectively. Thus, this process is promising for the further development of porous monovalent selective anion exchange membranes.

Received 15th June 2018
Accepted 13th July 2018

DOI: 10.1039/c8ra05152f

rsc.li/rsc-advances

1 Introduction

Membrane technology, which has a high water recovery rate and is environmentally friendly, is a key process in water treatment.[1–3] Electrodialysis (ED) is a promising membrane process to recover high value substances from water streams. ED is operated with a series of alternating cation-exchange and anion-exchange membranes arranged between a cathode and anode,[4] leading to the recovery of valuable substances from industrial wastewater and brackish water.[5–8] However, ED applications are often in complex and diversified water systems, aiming at *e.g.*, removing F^- or NO_3^- from groundwater in some poor areas, and the separation of SO_4^{2-} to avoid the undesirable formation of scale in the concentrating compartment during desalination. Therefore, highly efficient monovalent anion selective membranes are required to restrict the transport of multivalent anions and promote the migration of monovalent ions through the membrane structure.[8–12] In order to achieve an enhanced membrane performance, many research efforts have been devoted to investigating the mechanism for preparing high performance monovalent selective anion exchange membranes. The mechanism of these studies is principally focused on the difference of hydrated ionic radius and valence, based on the sieving and electrostatic repulsion, respectively.[8,13–16]

The most explored strategy is the modification of the membrane surface,[17,18] which is mainly dependent on the method of depositing a negatively or positively charged layer on the surface of a commercial anion exchange membrane or a lab-made anion exchange membrane.[8,14,16,19] For example, Shahi

[a]Center for Membrane Separation and Water Science & Technology, Ocean College, Zhejiang University of Technology, Hangzhou 310014, P. R. China. E-mail: shenjn@zjut.edu.cn; panjiefeng@zjut.edu.cn
[b]Huzhou Institute of Collaborative Innovation Center for Membrane Separation and Water Treatment, Zhejiang University of Technology, 1366 Hong Feng Road, Huzhou, Zhejiang, 313000, China
[c]Rey Juan Carlos University, 28942 Fuenlabrada, Madrid, Spain

† Electronic supplementary information (ESI) available. See DOI: 10.1039/c8ra05152f

et al.[19] found that a thin polypyrrole layer was useful to increase the permselectivity of a modified membrane (from 0.747 to 0.889). Mulyati *et al.*[20] proposed a method of using polyelectrolyte multilayer deposition on an anion exchange membrane. It was found that the modified membrane had a selectivity of 0.4 (SO_4^{2-} against Cl^-) after deposition of 15 layers. Zhao *et al.* fabricated a monovalent selective anion exchange membrane by the method of alternate electrodeposition polyelectrolyte on the surface of a commercial anion exchange membrane. The results showed that the permselectivity and separation efficiency of the modified anion membranes were all increased.[4,16,21]

To further reinforce the stability between the matrix and the modified layer, Zhang *et al.*[8] fabricated a monovalent anion permselective membrane (MASM) with a thin electronegative layer by the method of interfacial polymerization. The results indicated the modified membranes had a long-term operational stability and excellent permselectivity. Ruan *et al.*[22] fabricated a monovalent selective anion change membrane, which was modified a commercial anion exchange membrane by S-PDA (sulfonated polydopamine). The results stated the modified membranes had a permselectivity of 34.02 and stabilized in a long-term measurement.

In order to further meet the requirement of the industry, some researchers prepared the monovalent selective ion exchange membranes by using the method of internal substrate modification. Xu *et al.*[17] prepared a monovalent selective cation exchange membrane by using the polyvinyl alcohol (PVA) as matrix. The permselectivity (H^+ against Zn^{2+}) was improved by annealing treatment of the membrane to change its crystallinity. Pan *et al.*[4] prepared internally cross-linked monovalent selective anion exchange membranes by the method of one-pot. The prepared membranes had excellent permselectivity under different pH conditions, especially the permselectivity could be 24.55 at pH 10.

So above all, it is easy to know no matter surface modification or internal substrate modification, the modified membranes are all dense. So there is no reporting about the porous membranes using as monovalent anion selective membranes. In general, most monovalent anion selective membranes contain two layers: one is a dense anion exchange membrane as the substrate; the other is the active modified layer, which plays a core function for selective separation of monovalent and multivalent anions. When the substrate is replaced by a porous membrane, the resulting membrane would become a nanofiltration membrane alike. Moreover, nanofiltration is a pressure-driven process that can also achieve a separation between mono/multi-valent ions.[23,24] Nanofiltration membranes are often prepared *via* interfacial polymerization to form an active dense layer on a porous substance.[24,25] Recently, Ge *et al.*[3] proposed to use a lab-made nanofiltration membrane instead of a cation exchange membrane in conventional electrodialysis for fractionation of monovalent cations. The results indicated that the porous structure of the membrane could decrease the transfer resistance of ions, improving the flux of monovalent cations. Nevertheless, nanofiltration membranes are usually negatively charged,[26] which could limit their use as monovalent cation selective membranes in ED; so, a meaningful strategy could be to use them as a monovalent anion selective membrane, taking into account the electrostatic repulsion mechanism advantage. Therefore, inspired by their structures and surface characteristics, we prepared the nanofiltration membrane inspired asymmetric porous membrane for fractionation of monovalent anions in electrodialysis. Nevertheless, the stability of the compactness and the charge of membrane surfaces are major challenges, which require a key material (additive) to be used during membrane preparation.

Dopamine has been widely used for surface modification of various materials.[27] It can be oxidized, and it self-polymerizes under alkaline conditions to form a polydopamine (PDA) layer coatings with great adhesive strength. In addition, the presence of quinone groups in its chemical structure leads to a reaction with thiol-bearing compounds and nitrogen derivatives, enabling the chemical functionalization of the surface of a material.[27–31] Besides, dopamine can also be used for preparing monovalent selective anion membranes due to the dense structure or negative charge properties of the modified membrane surface.[9,32,33] These characteristics make PDA a good candidate material to control the compactness and the surface charge of these nanofiltration membranes inspired asymmetric porous membranes. In this study, a new application possibility is explored: nanofiltration membrane inspired asymmetric porous membranes were proposed as monovalent selective anion membranes in ED. These modified porous membranes with different compactness and charge properties were prepared by controlling the specific surface properties with a mussel-inspired "bio-glue" PDA layer and carboxylic polyamide layer. As illustrated in Fig. 1, it involved a simple deposition PDA layer on the surface of a PSf ultrafiltration membrane. Subsequently, the interfacial polymerization between piperazine (PIP) and trimesoyl chloride (TMC) was conducted to improve the upper layer density. Then, the carboxylation further enhances the surface electronegativity. The chemical constitution, structure and permselectivity of these modified porous membranes were discussed and investigated in detail.

2 Experimental

2.1 Materials and reagents

Polysulfone (PSf) ultrafiltration (UF) membranes were supplied by Hangzhou Water Treatment Technology Development Center (China). Commercial cation exchange membranes (Neosepta CEMs) were purchased from Fujifilm Corp., Japan. The characteristic properties of commercial cation exchange membranes are shown in Table 1. Dopaminehydrochloride, tris-(hydroxymethyl) aminomethane (Tris), piperazine (PIP, 99%), 1,3,5-benzenetricarbonyl trichloride (TMC, 99%), *n*-hexane, sodium chloride (NaCl, 99%) and sodium sulfate (Na_2SO_4, 99%) were all purchased from Aladdin Reagent Co. Ltd. (Shanghai, China).

2.2 Membrane preparation

Before membrane fabrication, the PSf ultrafiltration membranes used as substrate were firstly immersed in DI water

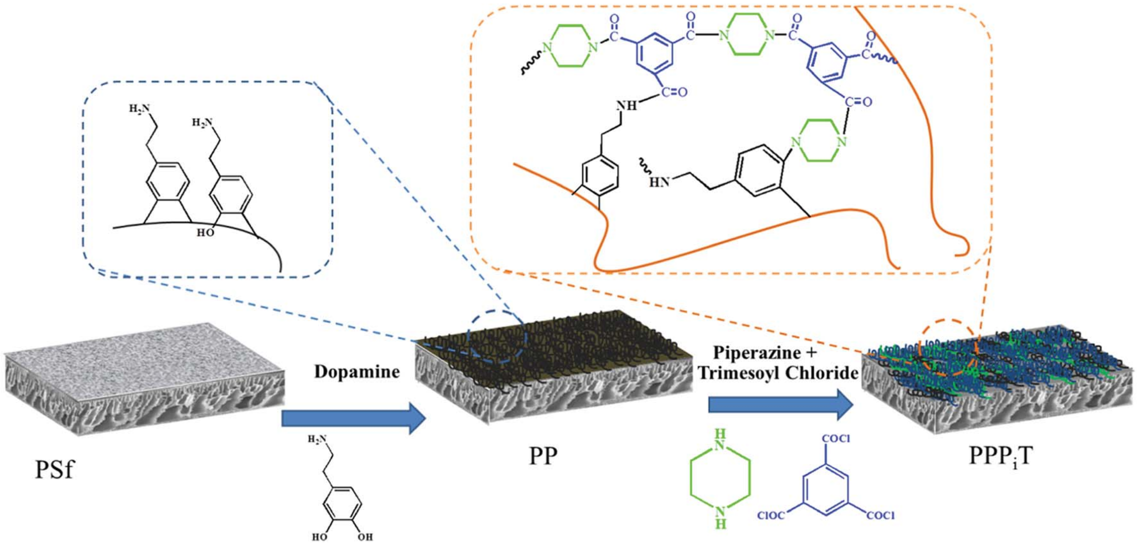

Fig. 1 Schematic illustration of the procedure for NF inspired asymmetric porous membrane preparation.

Table 1 Properties of the commercial CEMs used in this study

Membrane type	Thickness (μm)	Electrical area resistance (Ω cm^2)	pH stability
Homogeneous (CEM)	135	2.7	4–12

for 24 h, and then rinsed completely with DI water and air dried. The dopamine solution for surface coating was conducted by dissolving 0.2 g dopamine hydrochloride in 100 mL Tris–HCl buffer solution (pH 8.5). The coating process was conducted at room temperature by a custom-designed apparatus with three cells during 24 h to make sure the compacted structure, as shown in Fig. 2.[32,33] The effective membrane surface modified area was 28.26 cm^2. After PDA coating, the membranes were thoroughly washed with DI water to remove the unreacted chemicals and dried in the air. The resulting membrane was denoted as PP. Subsequently, the top surface of PP was immersed in 0.5% (w/v) TMC *n*-dodecane solution for 10 min. Subsequently, the membrane was rinsed twice with *n*-hexane to remove the excessive TMC. Then, the as-prepared TMC grafted membrane was immediately placed in an oven for 10 min to ensure the reaction between TMC and PDA at a fixed temperature of 60 °C. The resulting TMC crosslinked membrane was denoted as PPT.

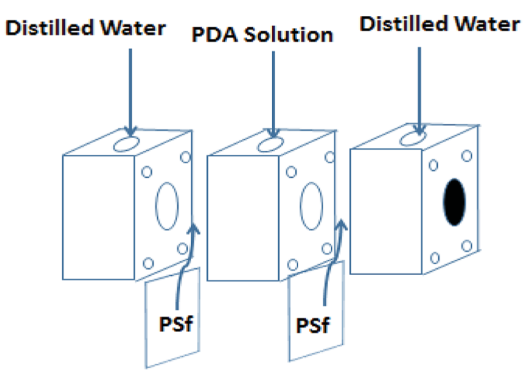

Fig. 2 Schematic drawing of PDA coating process.

In order to increase the density of the surface layer, the PP membrane was immersed in a 3 g L^{-1} piperazine (PIP) solution for 30 min; then the membrane was dried in an oven at 60 °C for 10 min. After that, the membrane was grafted with TMC, using the same process as for the PPT membrane formation. The final membrane was named PPP$_i$T. A conventional nanofiltration membrane was prepared *via* interfacial polymerization between trimesoyl chloride (TMC) and piperazine (PIP), and this membrane was named PP$_i$T. All TMC grafted composite membranes were immersed in DI water for around 24 h to hydrolyze the surface acylchloride groups to carboxyl groups.

2.3 Membrane characterization

2.3.1 FTIR characterization and X-ray photoelectron spectroscopy (XPS). To check whether modified materials have been grafted onto the surface of the PSf membranes, the chemical structure and elemental analysis of these different modified porous membranes were characterized by Fourier transform infrared spectroscopy (FTIR) and X-ray photoelectron spectroscopy (XPS). FTIR spectrum was recorded by using a FTIR spectrometer (Nicolet6700) and XPS was discussed by a XPS spectrometer (Kratos AXIS Ultra DLD, Japan).

2.3.2 Scanning electron microscopy (SEM) and atomic force microscopy (AFM) analysis. The morphology of these modified porous membranes was observed by scanning electron microscopy (SEM, SU8010, Hitachi, Japan). All samples were dried before measurement. The surface roughness values and both topographical and 3D images of these modified porous membranes were observed by atomic force microscopy (AFM, Germany). All samples were dried before measurement.

2.3.3 Contact angle measurement. The hydrophilcity of these modified porous membranes was obtained by measuring the water contact angle by a contact angle goniometer (OCA-20, Dataphysics, Germany). All samples were dried before measurement.

2.4 Measurements of electrochemical properties

2.4.1 Membrane surface resistance. The membrane surface resistance was obtained by using a commercial cell[34] as shown in Fig. 3. The electrode liquid was 0.5 M Na_2SO_4 in the electrode chamber and the middle chamber was filled with 0.5 M NaCl as measured liquid. The resistance of these modified porous membranes was calculated according to the following equation:

$$R_n = \frac{U - U_0}{I} \times S \tag{1}$$

where R_n is stand for the membrane surface resistance (Ω cm^2), U is stand for the voltage of the sample (V) and U_0 is the voltage value of without sample (V), I is the constant current (0.04 A), S is stand for the effective measurement area (7.065 cm^2).

2.4.2 ζ-potential measurements. The surface electrical properties of these modified porous membranes were characterized by an instrument (SurPASS3, AntonPaar, Austria) with 1 mM KCl as the electrolyte solution at pH 6.5.

2.5 Monovalent anion permselectivity measurements of modified porous membranes and electrodialysis

The permselectivity of NF inspired asymmetric porous membranes was investigated by a commercial ED apparatus with four cells and the volume of each cell is 100 mL, as shown in Fig. 4.[35] These prepared NF inspired asymmetric porous membranes were placed in the middle of the four cells. Crucially, the modified layer of these porous membranes was directed towards the cathode. The remaining two locations were clamped by two commercial cation exchange membranes towards the electrodes. Later, a solution of 0.05 M NaCl and 0.05 M $Na_2SO_4$was added into the two middle cells; the electrode cell was filled with 0.2 M Na_2SO_4.[36] The monovalent anion permselectivity measurements were carried out for 60 minutes at a current density of 5.1 mA cm^{-2}. In order to choose the appropriate current density, the permselectivity measurements under different current density conditions were conducted out (the Fig. S1 in the ESI†). After 60 min, the concentration of the solution in the dilute cell was measured by Anion Chromatography (Thermo Fisher ICS-1100).[4]

To further indicate the change of ion concentrations (Cl^- and SO_4^{2-}) with time in the dilute cell by using a PPP$_i$T membrane as a temple, a two hours electrodialysis measurement was conducted in the same commercial ED apparatus (Fig. 4). The ED experiment was conducted for 120 minutes at the current density of 5.1 mA cm^{-2}, and the concentration of the solution in the dilute cell was measured by same Anion Chromatography after 20 min, 40 min, 60 min, 80 min, 100 min, and 120 min.

The permselectivity of the membranes was calculated by the following equation:[4,16]

$$P_{SO_4^{2-}}^{Cl^-} = \frac{t_{Cl^-} / t_{SO_4^{2-}}}{c_{Cl^-} / c_{SO_4^{2-}}} = \frac{J_{Cl^-} c_{SO_4^{2-}}}{J_{SO_4^{2-}} c_{Cl^-}} \tag{2}$$

where t_i is the transport number of different ions, J_i is the flux of the ions and c is the concentration of the solution in the dilute cell. The parameter t_i was calculated using following the equation:

$$t_i = \frac{J_i z_i F}{I} \tag{3}$$

where z_i is the ion charge, F is Faraday's constant and I is the current.

The flux of ions was obtained from the change in concentration of the ions on the dilute side according to:

$$J_i = \frac{V \frac{dc_i}{dt}}{A} \tag{4}$$

where V is the volume of the electrolyte solution in the dilute compartment (100 mL), and A is the active area (19.625 cm^2).

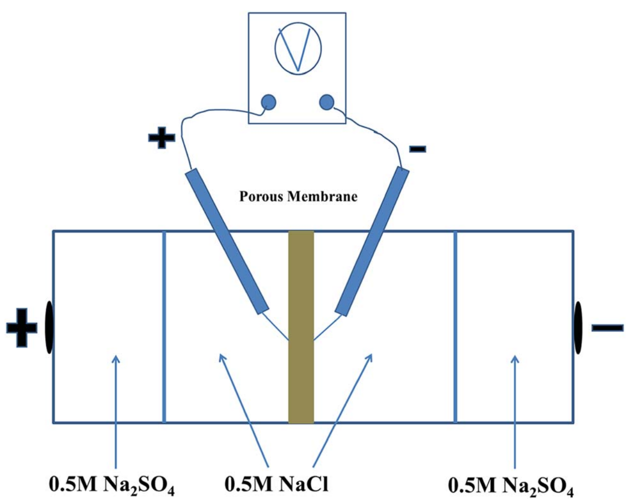

Fig. 3 Schematic drawing of a four-electrode mode commercial measurement module for membrane resistance.

3 Results and discussion

3.1 Chemical structure and composition of modified porous membranes

NF inspired asymmetric porous membranes were prepared *via* a reaction between acylchloride groups and amines from PIP or PDA sources (Fig. 1) by interfacial polymerization. The chemical structure and elemental distribution of these modified porous membranes were investigated by using FTIR and XPS.

The FTIR spectra results of PSf, PP$_i$T, PP, PPT, and PPP$_i$T membranes are shown in the Fig. 5. The absorption bands at 1627 cm^{-1} are due to the C=C bond vibration of aromatic rings (Fig. 5 PP) or vibration band of the amide C=O groups (Fig. 5 PP$_i$T, PPT and PPP$_i$T).[37] The comparison between the obtained spectra for modified membranes with the pristine PSf indicates the existence of PDA on the PP membrane surface. In addition, new peaks at 1727 cm^{-1} (Fig. 5 PP$_i$T, PPT and PPP$_i$T, not appearing in PP), are due to the stretching vibration band of the carboxyl C=O groups,[38] which proves the successful interfacial polymerization, and also shows that after TMC grafting there were unreacted acyl chloride groups on the surface of the

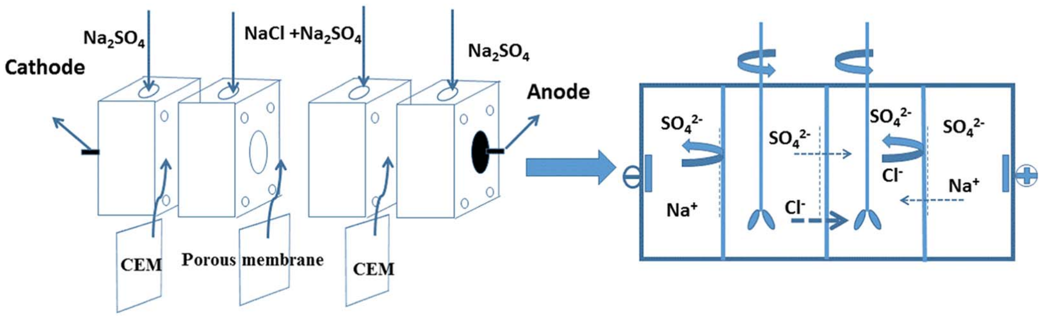

Fig. 4 Schematic drawing of a four-electrode mode for monovalent anion permselectivity measurement.

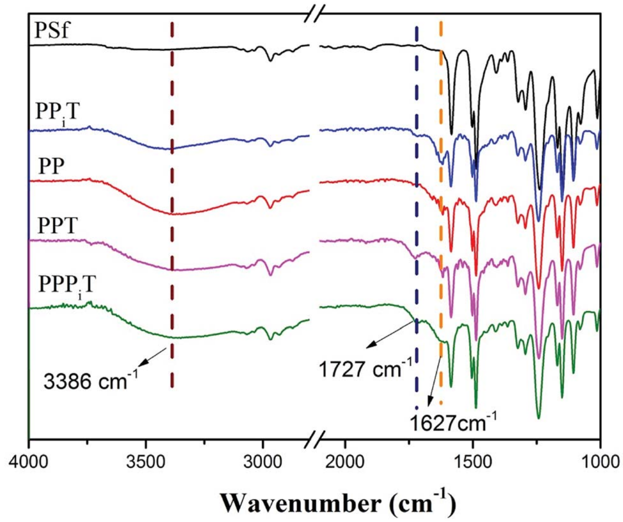

Fig. 5 FTIR spectra of the tested membranes.

membranes. Bands at 3386 cm^{-1}, assigned to the vibration of the O–H bond, suggest the presence of hydrophilic amine groups, or carboxyl groups due to the hydrolysis of the acyl chloride groups.

To determine the surface chemical properties, XPS was used with about 10 nm detection effective depth limit.[23,39] Fig. 6 and Table 2 show the XPS spectra of PSf, PP$_i$T, PP, PPT and PPP$_i$T membranes, and their surface elemental composition. For comparison, the main corresponding elements (C, O, N, S) of these modified porous membranes were measured under the same conditions. Compared with PSf, the PP$_i$T membrane exhibits a high content of nitrogen (N) (7.88 ± 0.24% *vs.* 2.85 ± 0.06%), as well as a high content of oxygen (O) (20.48 ± 1.02% *vs.*17.23 ± 0.86%). The higher content of O is mainly attributed to the unreacted acyl chloride groups changing into carboxyl groups by hydrolysis. In contrast, the sulfur (S) content dropped from 2.21% to 0.89 as a result of the formation of a polyamide layer on the surface of the PP$_i$T membrane. All these results prove the reaction between PIP and TMC and the successful interfacial polymerization process. The N content of the PP membrane increased from 2.85 ± 0.06% (PSf membrane) to 7.61 ± 0.15%. A higher C/N molar ratio of 0.112 and a lower S content of 1.06 were obtained. These results show the successful formation of PDA layer over the PSf substrate. Then, after TMC grafting and subsequent hydrolysis treatment, the atomic ratio of O/N increases up to 3.969 for the PPT membrane, as shown in Table 1. Moreover, the O content increases from 24.86 ± 0.75% for the PP membrane up to 25.88 ± 1.03% for the PPT membrane, as a result of the introduction of carboxylic groups formed from the hydrolysis of unreacted acyl chlorides. However, the sulfur 2p signal as shown in Fig. 6(d) is still detected on the PPT membrane surface, but the value decreases from 1.06 ± 0.03% to 0.6 ± 0.01%. This effect can be attributed to the increment of membrane thickness due to the TMC grafting.

Therefore, after PIP deposition and TMC grafting, the nitrogen 1s signal of the PPP$_i$T membrane shown in Fig. 6(e) is stronger than that of the PPT membrane, while the nitrogen content as well as the N/C ratio notably increased from 6.52 ± 0.32% to 6.89 ± 0.22%, and from 0.098 to 0.101 respectively. In addition, the O content decreases from 25.88 ± 1.03% to 23.73 ± 0.44%, because of the presence of PIP molecules onto the PP membrane surface deposited *via* Michael addition.

3.2 SEM and AFM analysis

The surface and cross-section SEM morphologies of these modified porous membranes are shown in Fig. 7. It can be indicated the PDA modified membrane exhibited a relatively smooth surface (Fig. 7c) compared with others modified membranes. Moreover, small PDA nanoparticles formed during

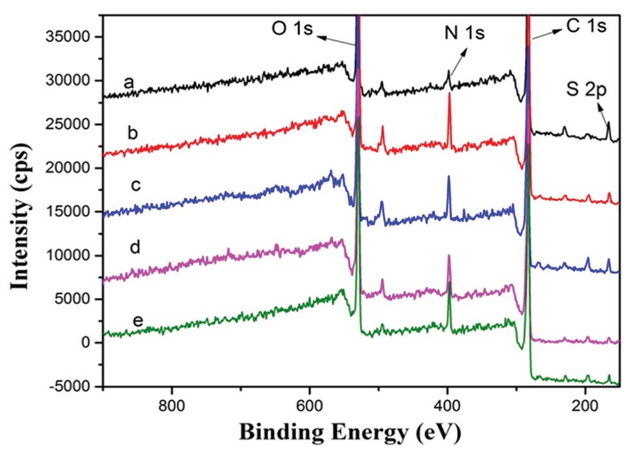

Fig. 6 XPS spectra of PSf (a), PP$_i$T (b), PP (c), PPT (d), PPP$_i$T (e) membrane surfaces.

Table 2 XPS elemental analyses of PSf, PP_iT, PP, PPT and PPP_iT membranes

Sample	C 1s (%)	N 1s (%)	O 1s (%)	S 2p (%)	N/C	O/N
PSf	77.18 ± 2.3	2.85 ± 0.06	17.23 ± 0.86	2.21 ± 0.04	0.037	6.045
PP_iT	70.2 ± 3.5	7.88 ± 0.24	20.48 ± 1.02	0.89 ± 0.02	0.112	2.599
PP	65.50 ± 1.9	7.61 ± 0.15	24.86 ± 0.75	1.06 ± 0.03	0.116	3.267
PPT	66.53 ± 1.3	6.52 ± 0.32	25.88 ± 1.03	0.6 ± 0.01	0.098	3.969
PPP_iT	68.14 ± 1.0	6.89 ± 0.22	23.73 ± 0.44	0.77 ± 0.01	0.101	3.444

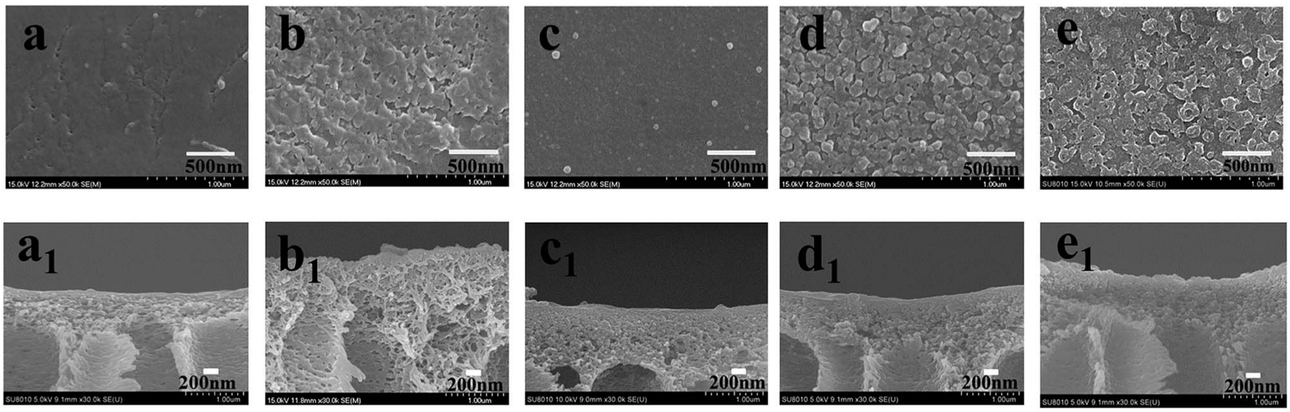

Fig. 7 Surface sectional SEM micrographs of PSf (a), PP_iT (b), PP (c), PPT (d) and PPP_iT (e); cross sectional SEM micrographs of PSf (a_1), PP_iT (b_1), PP (c_1), PPT (d_1) and PPP_iT (e_1).

the oxidation process of dopamine also appeared on the PP membrane. The membranes modified by interfacial polymerization (Fig. 7b, d and e) show a typical nodular structure, mainly resulting from the cross-linking of reactive monomers of PIP, PDA and TMC. The cross-sectional morphologies of PSf, PP_iT, PP, PPT and PPP_iT membranes are shown in Fig. $7a_1$–e_1. The PSf membrane (Fig. $7a_1$) displays a type of asymmetric membrane morphology by the composition of a skin layer on the top and a finger-like porous layer at the bottom. No large morphological changes between the PSf membrane (Fig. $7a_1$) and the modified membrane were observed, indicating that the PDA coating procedure did not considerably alter the structure of the PSf support layer. As shown in Fig. $7b_1$, d_1 and e_1 a dense polyamide layer was formed on the PP_iT, PPT and PPP_iT membrane after TMC coating. It is difficult to distinguish the polyamide layer of the skin layer and the support layer in these membranes, which indirectly suggests a good adhesion between the modified support and the polyamide layer.[37]

Fig. 8 shows the three-dimensional (3D) AFM surface images of PSf, PP_iT, PP, PPT and PPP_iT membranes. It can be found that the PP_iT membrane has the highest average roughness (R_a) in comparison with other membranes. In addition, the PDA modified membranes have the lowest value of R_a, which is very consistent with the SEM images (Fig. 7). After PDA addition, the R_a value shows a significant reduction from 59.4 to 9.22 and 11.0 (Fig. 8d and e) compared with the conventional interfacial polymerization membrane (PP_iT). From Fig. 8a, it can be seen that the PSf membrane surface has a high roughness with several obvious "peaks" and "valleys", so after PDA coating, the particles of PDA can fill the valleys of the PSf membrane smoothen the surface of the PP membrane.[38] Nevertheless, after PIP and TMC coating, the average roughness (R_a) increased to 9.22 nm for PPT and 11.0 nm for the PPP_iT membrane. Moreover, the different roughness values estimated for the PP, PPT and PPP_iT membranes are in agreement with the surface structures of these membranes observed by SEM (Fig. 7(c)–(e)).

3.3 ζ-potential and contact angle

Surface charge properties are very important for monovalent anion selective membranes. Nanofiltration inspired porous membranes with negatively charged surfaces were prepared and designed to improving the permselectivity. For this reason, the surface charged properties and hydrophilicity of these porous membranes were investigated by the ζ-potential and water contact angle, as shown in Fig. 9 and 10.

Fig. 9 presents the ζ-potential of the PSf, PP_iT, PP, PPT and PPP_iT membranes at pH 6.5. All these modified porous membranes emerge a negative ζ-potential because of the presence of negative charged functional (hydroxyl or carboxyl) groups on the membrane surface. The membranes modified by TMC show a stronger negative charge than PDA modified membranes, due to the weaker negative charge of phenolic hydroxyl groups (PDA) compared with carboxylic groups (TMC). The PP membrane was successively coated by PIP and TMC, and the ζ-potential value significantly increased to −41.29 mV for the PPP_iT membrane. This variation could be attributed to the increment of the amount of carboxylic groups as a result of the addition of PIP, which was demonstrated by ATR-IR in Fig. 5. Moreover, the ζ-potential of PP_iT membrane is higher than

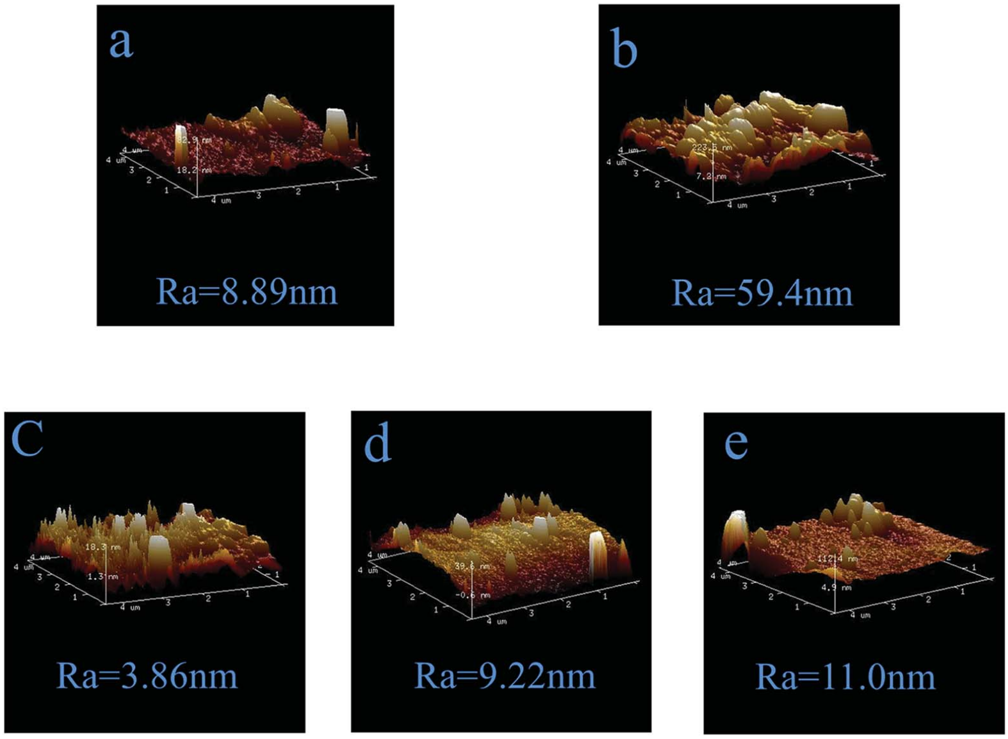

Fig. 8 AFM micrographs of PSf (a), PP_iT (b), PP (c), PPT (d) and PPP_iT (e).

PPP_iT membrane, because of the existence of negative PDA layer on the PPP_iT membrane.

The water contact angle is a very important parameter to describe the surface hydrophilicity of membranes. The water contact angle values of these different modified porous membranes are shown in Fig. 10. The bare PSf has the highest contact angle due to its relatively hydrophobic character. However, after PDA modification, the contact angle decreased from 74.1° for the PSf membrane to 61.9° for the PP membrane, which suggesting an improved membrane hydrophilicity as a result of PDA coating, because of hydrophilic groups occurring onto the PDA layer. Moreover, when the PP membrane was successively coated with PIP and TMC, the water contact angle decreased to 51.4° for the PPP_iT membrane. As result of the interfacial polymerization reaction between PDA layer, PIP layer and TMC, more hydrophilic groups are formed on the surface of the modified membrane. As for the traditional interfacial polymerization modified PP_iT membrane that has the lowest water contact angle value of 45.8°, which indicates the most hydrophilic groups are formed on the surface of it. All the observed changes in the surface characteristics of the tested membranes (ζ-potential and hydrophilicity) confirm the success of the membrane surface modifications.

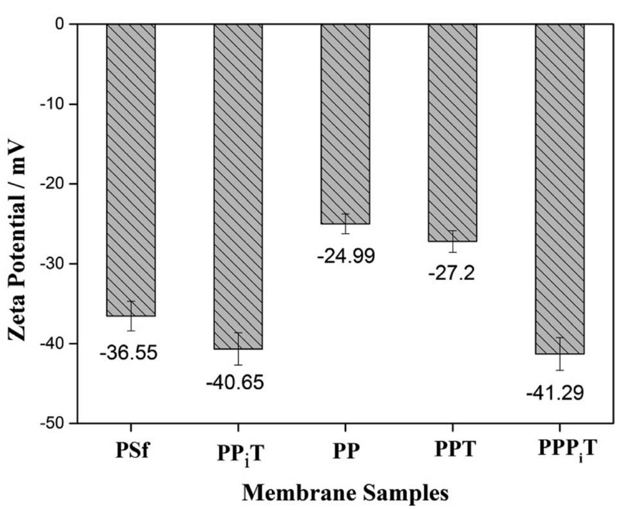

Fig. 9 The ζ-potential of different membranes at pH round 6.5.

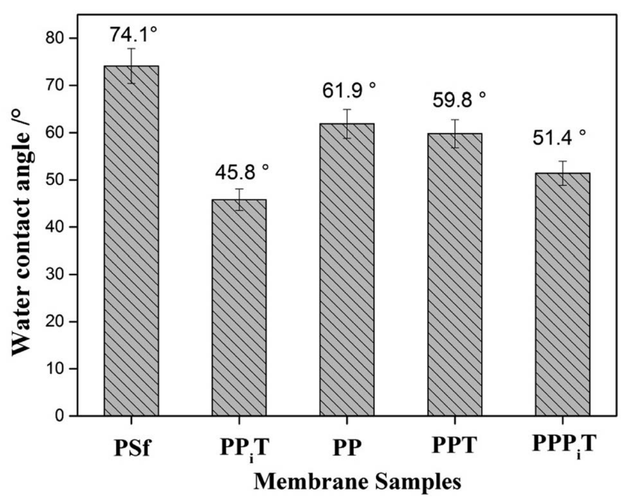

Fig. 10 The water contact angle for different types of membrane.

3.4 Membrane resistance

The membrane resistance is a parameter of great concern for ion exchange membranes performance. These materials are usually made of a polymer backbone carrying ion exchange groups; the membrane resistance enhances with decreasing ion exchange groups. As for anion exchange membranes, the ion exchange groups are usually quaternary ammonium groups.[40] However, the modified membranes used in this work consist of a porous PSf membrane and a dense top layer, so there are no ion exchange groups in the chemical structure of these membranes. Therefore, the membrane resistance values of those membranes are relatively higher than those of traditional anion exchange membranes (the membrane resistance could be decreased by decreasing the thickness of modified layers and based membranes). Fig. 11 shows the membrane resistance values obtained for membranes tested in this work. The bare membrane (PSf membrane) has the lowest membrane resistance of 8.84 Ω cm^2 compared to the other four membranes, but is still higher than that of a conventional homogeneous AEM membrane because it is an uncharged porous UF membrane. Moreover, the membrane resistance distinctly increases from 8.84 Ω cm^2 for the PSf membrane to 11.48 Ω cm^2 for the PP membrane after PDA coating. The increasement of membrane resistance is mainly belonged to the existence of a dense and negatively charged PDA layer on the surface of the membrane under alkaline and aerobic conditions. The PDA layer favors the migration of monovalent anions through the membrane but hinders the multi-valent anions.[9,32] However, after TMC coating, the membrane resistance decreased from 11.48 Ω cm^2 for the PP membrane to 10.42 Ω cm^2 for the PPT membrane. It is expected that as a result of the TMC coating the membrane surface became denser, leading to an increase of the membrane resistance. However, the presence of unreacted acyl chloride groups with negative charged carboxylic acid groups in its chemical structure promotes the transport of cations, affecting negatively the membrane resistance. Moreover, the membrane resistance mildly increases from 10.42 Ω cm^2 for PPT to 11.39 Ω cm^2 for the PPP$_i$T membrane, which indicates that a much denser layer of PPP$_i$T is formed after coating with PIP and TMC. As for the TFC membrane (PP$_i$T), which is prepared by interfacial polymerization, the highest membrane resistance (13.42 Ω cm^2) is observed because of the increased thickness and the amount of the modified layers added (Fig. 7b and b$_1$).

3.5 Mono/multi-anion selectivity

To indicate the differences in anion mobility among these modified porous membranes in this work, they were tested by electrodialysis a NaCl/Na_2SO_4 mixed solution. The permselectivity $\left(P^{Cl^-}_{SO_4^{2-}}\right)$ of the surface modified porous membranes is shown in Fig. 12. Under the same experiment condition, the permselectivity of commercial monovalent selective anion exchange membrane (NEOSEPTA® ACS were purchased from ASTOM Corp., Japan) is 10.86 (although, it is higher than the optimized membrane (3.1), the work is still meaningful for experiment research). On the one hand, it is clear that all modified porous membranes have an excellent permselectivity ranging from 1.42 for PP$_i$T to 3.1 for PPP$_i$T. This effect demonstrates the feasibility and validity of modified porous membranes to be used as monovalent selective anion membranes. On the other hand, for the modified membrane based on PDA, the PPP$_i$T membrane showed a higher permselectivity $\left(P^{Cl^-}_{SO_4^{2-}} = 3.1\right)$ in comparison with the PPT membrane $\left(P^{Cl^-}_{SO_4^{2-}} = 2.41\right)$ and the PP membrane $\left(P^{Cl^-}_{SO_4^{2-}} = 1.79\right)$. This can mainly be ascribed to surface charge properties (zeta potential), displayed in Fig. 9, which determine the permselectivity of the membranes illustrated in Fig. 12. The increment of the active layer density could be an additional reason to explain the observed permselectivity increase. Compared with the PP membrane, the modification proposed for PPT and PPP$_i$T membranes yield a much denser structure of the active layer for improving the permselectivity, as shown in Fig. 7. Therefore, as result of the synergistic effect of the sieving mechanism and electrostatic repulsion, the PPP$_i$T membrane

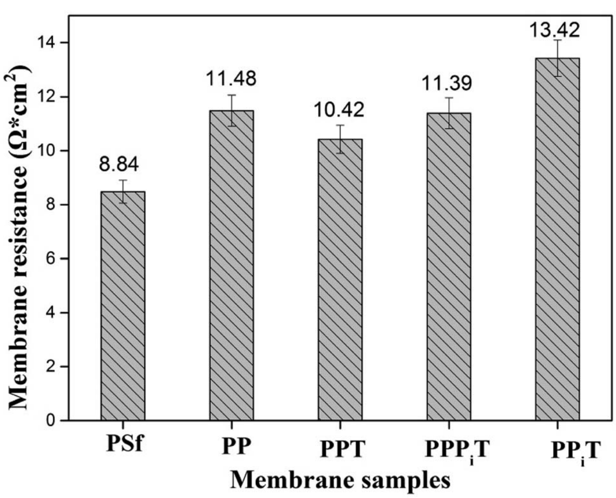

Fig. 11 The membrane resistance values of different membranes.

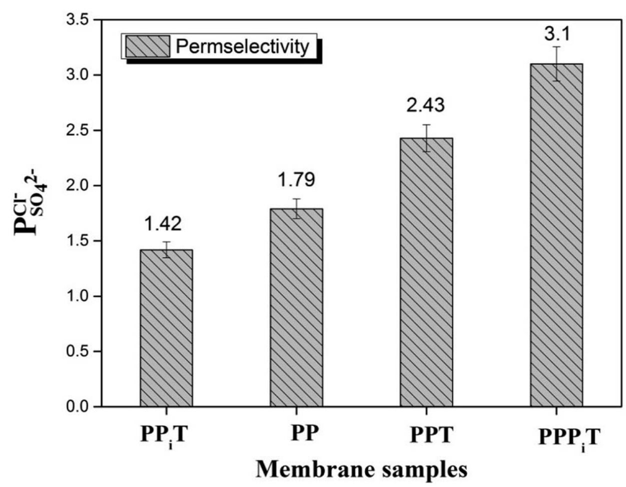

Fig. 12 The permselectivity coefficient of chlorine ion against sulfate ion of different membranes at time of one hour.

has the highest permselectivity $\left(P^{Cl^-}_{SO_4^{2-}}\right)$. Thirdly, it is interesting to note that the modified porous membrane (PP_iT) based on TMC and PIP by conventional interfacial polymerization has a lower permselectivity than the modified membranes based on PDA, although the former membrane has an even more negative charge. The upper layer density determines the enhanced permselectivity of the modified membranes. The conventional membrane preparation procedure based on the interfacial polymerization endows the active layer with a loose structure,[41] as shown in Fig. 7b and 8b. Furthermore, the modified porous membranes are chosen as monovalent selective anion membranes in order to benefit from the synergistic effect of sieving and electrostatic repulsion mechanism.

To further indicate the permselectivity performance of these modified porous membranes, the optimized membrane (PPP_iT) was used a sample to conduct a two hours electrodialysis experiment. The Cl^- and SO_4^{2-} concentration of the dilute compartment along with time by using the mixed anions solution (Cl^-/SO_4^{2-}) are shown in the Fig. 13. It is easy to find that the SO_4^{2-} concentration is always higher than the Cl^- concentration in the dilute cell at the same time during the electrodialysis process, which indicates that NF membrane inspired asymmetric porous membranes are potential to use as monovalent selective anion exchange membranes in ED process.

Meanwhile, the change of ion concentration in the dilute cell also indicates the modified porous membranes have the ability of desalination. The mechanism of the desalination performance is described that: as we all know, the ED is conducted by a series of alternating cation-exchange and anion-exchange membranes arranged between cathode and anode, with the help of electricity to realize purpose of desalination. Nevertheless, in this work the membranes used in the ED process are porous and non-ion exchange membranes. From the Fig. 13, it is easy to find that these porous modified membranes used in the ED process have the ability of desalination. Because these modified membranes have porous structure, which is profitable to transmit the ions and increase the ion flux. Moreover, these porous membranes were modified by the a mussel-inspired "bio-glue" PDA layer and carboxylic polyamide layer, so the presence of unreacted acyl chloride groups with negative charged carboxylic acid groups in its chemical structure are used as ion exchange groups to increase the ability of desalination performance, which is proved by the decrement of the membrane resistance (Fig. 11, PPT).

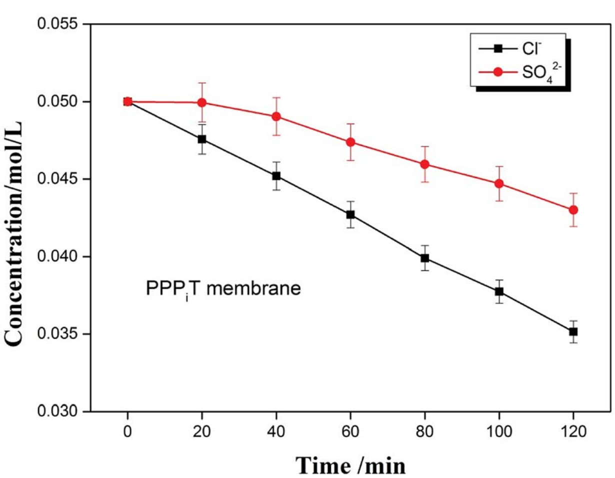

Fig. 13 Time-dependent concentration of Cl^- and SO_4^{2-} in the dilute compartment during ED.

4 Conclusions

New NF membrane inspired asymmetric porous membranes were prepared for being used as monovalent selective anion membranes. Membranes were prepared by controlling the specific surface properties with a mussel-inspired "bio-glue" PDA layer and a dense polyamide layer. In order to evaluate the monovalent anion selectivity of these modified porous membranes, ED operation for a Cl^-/SO_4^{2-} mixture was studied. The results show that these modified porous membranes exhibit an excellent monovalent anion permselectivity, influenced substantially by the membrane surface properties. The permselectivity of the asymmetric porous membrane modified by adding a PDA layer and a dense polyamide layer leads to a more than two-fold improvement in performance $\left(P^{Cl^-}_{SO_4^{2-}} = 3.1\right)$, compared with the conventional membrane by interfacial polymerization of piperazine (PIP) and trimesoyl chloride (TMC) $\left(P^{Cl^-}_{SO_4^{2-}} = 1.42\right)$. This synergistic interaction between the sieving mechanism and electrostatic repulsion is a key parameter for the selective transport of monovalent/multivalent anions. Moreover, this work would give us more inspiration to fabricate porous monovalent selective anion exchange membranes in the future.

Conflicts of interest

There are no conflicts to declare.

Acknowledgements

We thank the funding support from the Natural Science Foundation of China (No. 21676249), National Key Research and Development Plan (No. 2017YFC0403701) and Project for Assistance of Qinghai from Science Technology Department of Zhejiang Province (No. 2018C26004).

References

1 Y. Lv, Y. Du, W. Z. Qiu and Z. K. Xu, *ACS Appl. Mater. Interfaces*, 2017, **9**, 2966–2972.
2 P. Sun, R. Ma, W. Ma, J. Wu, K. Wang, T. Sasaki and H. Zhu, *NPG Asia Mater.*, 2016, **8**, e259.
3 L. Ge, B. Wu, Q. Li, Y. Wang, D. Yu, L. Wu, J. Pan, J. Miao and T. Xu, *J. Membr. Sci.*, 2016, **498**, 192–200.
4 J. Pan, J. Ding, Y. Zheng, C. Gao, B. Van der Bruggen and J. Shen, *J. Membr. Sci.*, 2018, **553**, 43–53.
5 Q. Pan, M. M. Hossain, Z. Yang, Y. Wang, L. Wu and T. Xu, *J. Membr. Sci.*, 2016, **515**, 115–124.

6 R. K. Nagarale, G. S. Gohil and V. K. Shahi, *Adv. Colloid Interface Sci.*, 2006, **119**, 97–130.
7 G. Loget, J. Roche and A. Kuhn, *Adv. Mater.*, 2012, **24**, 5111–5116, 5144.
8 H. Zhang, R. Ding, Y. Zhang, B. Shi, J. Wang and J. Liu, *Desalination*, 2017, **410**, 55–65.
9 M. Vaselbehagh, H. Karkhanechi, R. Takagi and H. Matsuyama, *J. Membr. Sci.*, 2015, **490**, 301–310.
10 X.-l. Wang, M. Wang, Y.-x. Jia and B.-b. Wang, *Electrochim. Acta*, 2015, **174**, 1113–1121.
11 T. Xu, *J. Membr. Sci.*, 2005, **263**, 1–29.
12 Z. Amora, S. Malkia, M. Takya and B. Barioub, *Desalination*, 1998, **120**, 263–271.
13 B. Tansel, *Sep. Purif. Technol.*, 2012, **86**, 119–126.
14 T. Sata, *J. Membr. Sci.*, 2000, **167**, 1–31.
15 R. Takagi, M. Vaselbehagh and H. Matsuyama, *J. Membr. Sci.*, 2014, **470**, 486–493.
16 J. Pan, J. Ding, R. Tan, G. Chen, Y. Zhao, C. Gao, B. V. der Bruggen and J. Shen, *J. Membr. Sci.*, 2017, **539**, 263–272.
17 L. Ge, L. Wu, B. Wu, G. Wang and T. Xu, *J. Membr. Sci.*, 2014, **459**, 217–222.
18 C. H. Park, S. Y. Lee, D. S. Hwang, D. W. Shin, D. H. Cho, K. H. Lee, T. W. Kim, T. W. Kim, M. Lee and D. S. Kim, *Nature*, 2016, **532**, 480.
19 G. S. Gohil, V. V. Binsu and V. K. Shahi, *J. Membr. Sci.*, 2006, **280**, 210–218.
20 S. Mulyati, R. Takagi, A. Fujii, Y. Ohmukai and H. Matsuyama, *J. Membr. Sci.*, 2013, **431**, 113–120.
21 Y. Zhao, K. Tang, H. Liu, B. Van der Bruggen, A. Sotto Díaz, J. Shen and C. Gao, *J. Membr. Sci.*, 2016, **520**, 262–271.
22 H. Ruan, Z. Zheng, J. Pan, C. Gao, B. Van der Bruggen and J. Shen, *J. Membr. Sci.*, 2018, **550**, 427–435.
23 T. Wang, H. Qiblawey, E. Sivaniah and A. Mohammadian, *J. Membr. Sci.*, 2016, **511**, 65–75.
24 A. W. Mohammad, Y. H. Teow, W. L. Ang, Y. T. Chung, D. L. Oatley-Radcliffe and N. Hilal, *Desalination*, 2015, **356**, 226–254.
25 Y. Lv, H.-C. Yang, H.-Q. Liang, L.-S. Wan and Z.-K. Xu, *J. Membr. Sci.*, 2015, **476**, 50–58.
26 T. Wang, Y. Yang, J. Zheng, Q. Zhang and S. Zhang, *J. Membr. Sci.*, 2013, **448**, 180–189.
27 H. Lee, S. M. Dellatore, W. M. Miller and P. B. Messersmith, *Science*, 2007, **318**, 426–430.
28 S. Hong, Y. S. Na, S. Choi, I. T. Song, W. Y. Kim and H. Lee, *Adv. Funct. Mater.*, 2012, **22**, 4711–4717.
29 J. Liebscher, R. Mrówczyński, H. A. Scheidt, C. Filip, N. D. Hădade, R. Turcu, A. Bende and S. Beck, *Langmuir*, 2013, **29**, 10539–10548.
30 Y. Liu, K. Ai and L. Lu, *Chem. Rev.*, 2014, **114**, 5057.
31 Q. Liu, N. Wang, J. Caro and A. Huang, *J. Am. Chem. Soc.*, 2013, **135**, 17679–17682.
32 M. Vaselbehagh, H. Karkhanechi, R. Takagi and H. Matsuyama, *J. Membr. Sci.*, 2016, **515**, 98–108.
33 M. Vaselbehagh, H. Karkhanechi, S. Mulyati, R. Takagi and H. Matsuyama, *Desalination*, 2014, **332**, 126–133.
34 B. Han, J. Pan, S. Yang, M. Zhou, J. Li, A. Sotto Díaz, B. Van der Bruggen, C. Gao and J. Shen, *Ind. Eng. Chem. Res.*, 2016, **55**, 7171–7178.
35 Y. Zhao, K. Tang, Q. Liu, B. V. D. Bruggen, A. S. Díaz, J. Pan, C. Gao and J. Shen, *RSC Adv.*, 2016, **6**, 16548–16554.
36 Y. Zhao, K. Tang, H. Ruan, L. Xue, B. Van der Bruggen, C. Gao and J. Shen, *J. Membr. Sci.*, 2017, **536**, 167–175.
37 Y. Li, Y. Su, J. Li, X. Zhao, R. Zhang, X. Fan, J. Zhu, Y. Ma, Y. Liu and Z. Jiang, *J. Membr. Sci.*, 2015, **476**, 10–19.
38 J. Jin, K. Zhang, X. Du and J. Yang, *J. Appl. Polym. Sci.*, 2017, **134**, 44430–44436.
39 Y. Li, Y. Su, X. Zhao, X. He, R. Zhang, J. Zhao, X. Fan and Z. Jiang, *ACS Appl. Mater. Interfaces*, 2014, **6**, 5548–5557.
40 J. Ran, L. Wu, Y. He, Z. Yang, Y. Wang, C. Jiang, L. Ge, E. Bakangura and T. Xu, *J. Membr. Sci.*, 2017, **522**, 267–291.
41 X. Zhang, Y. Lv, H. C. Yang, Y. Du and Z. K. Xu, *ACS Appl. Mater. Interfaces*, 2016, **8**, 32512–32519.